CHEMISTRY
A EUROPEAN JOURNAL

DOI: 10.1002/chem.200800716

One-Electron-Reduced and -Oxidized Stages of Donor-Substituted 1,1,4,4-Tetracyanobuta-1,3-dienes of Different Molecular Architectures

Milan Kivala,[a] Tsvetanka Stanoeva,[b] Tsuyoshi Michinobu,[a] Brian Frank,[a] Georg Gescheidt,*[b] and François Diederich*[a]

Abstract: A series of monomeric and oligomeric donor-substituted 1,1,4,4-tetracyanobuta-1,3-dienes (TCBDs) with various topologies have been synthesized by means of thermal [2+2] cycloaddition between tetracyanoethylene (TCNE) and donor-substituted alkynes, followed by retro-electrocyclization. One-electron-reduced and -oxidized stages of the donor-substituted TCBDs were generated by chemical methods. The obtained radical anions and radical cations were studied by using electron paramagnetic resonance/electron nuclear double resonance (EPR/ENDOR) spectroscopy, supported by density functional theory (DFT) calculations. The extent of π-electron delocalization in the paramagnetic species was investigated in terms of the EPR parameters. Despite favorable molecular orbital (MO) coefficients, the EPR results suggest that in radical anions the spin and charge are confined to the electron-withdrawing TCBD moieties on the hyperfine EPR timescale. The observed spin localization is presumably caused by an interplay between the nonplanarity of the studied π systems, limited π-electron conjugation, and very likely counterion effects. In radical cations, an analogous spin and charge localization confined to the electron-donating *N*,*N*-dialkylaniline moieties was found. In this case, an efficient electron delocalization is disabled by small MO coefficients at the joints between the donor and acceptor portions of the studied TCBDs.

Keywords: charge transfer · conjugation · cycloaddition · donor–acceptor systems · EPR spectroscopy

Introduction

Over the decades, organic electron donor–acceptor (D–A)-substituted systems, featuring intramolecular charge-transfer interactions, have attracted considerable interest as promising candidates for use in next-generation electronic and optoelectronic devices.[1,2] Furthermore, bimolecular D–A architectures, capable of undergoing intermolecular charge transfer, have been utilized for the development of molecular organic conductors.[3,4] Organic materials are of particular attraction due to the ease of structural tuning to enhance specific properties for specialized applications, such as third-order nonlinear optical (NLO) effects.[5]

Recently, we introduced a new class of potent charge-transfer (CT) chromophores, donor-substituted 1,1,4,4-tetracyanobuta-1,3-dienes (TCBDs),[6,7] accessible in very high yields in an atom-economic synthesis by formal [2+2] cycloaddition between tetracyanoethylene (TCNE) and donor-substituted alkynes, followed by retro-electrocyclization.[8] Observed large third-order optical nonlinearities together with high stability and easy synthetic accessibility make these compounds attractive for fabrication of optoelectronic devices.[6,9] Despite substitution with *N*,*N*-dialkylanilino, methoxyphenyl, or thienyl donors, the TCBD moiety in these systems remains a potent electron acceptor. Particularly remarkable are the electrochemical properties of oligomeric and dendritic donor-substituted TCBDs, which undergo several reversible electron-transfer processes under electrochemical conditions.[7] These systems were shown to act as "molecular batteries", featuring exceptional electron uptake and storage capacity.[10]

Herein, we report an initial investigation of one-electron-reduced and -oxidized stages of monomeric and oligomeric

[a] Dr. M. Kivala, Dr. T. Michinobu, B. Frank, Prof. Dr. F. Diederich
Laboratorium für Organische Chemie, ETH-Hönggerberg
Wolfgang-Pauli-Strasse 10, 8093 Zürich (Switzerland)
Fax: (+41) 44-632-1109
E-mail: diederich@org.chem.ethz.ch

[b] T. Stanoeva, Prof. Dr. G. Gescheidt
Institut für Physikalische und Theoretische Chemie, TU Graz
Technikerstrasse 4/I, 8010 Graz (Austria)
Fax: (+43) 316-873-8225
E-mail: g.gescheidt-demner@tugraz.at

Supporting information for this article is available on the WWW under http://dx.doi.org/10.1002/chem.200800716.

donor-substituted TCBDs **1**–**9** by means of electron paramagnetic resonance/electron nuclear double resonance (EPR/ENDOR) spectroscopy, supported by density functional theory (DFT) calculations, to probe the extent of electronic interaction between the D–A dyads within a molecule when an electron is either added or removed.

Results and Discussion

Topology: Donor-substituted TCBD derivatives **1**–**9** can be divided into three different classes depending on their structural features. Molecules **1**–**4** are monomeric, composed of a 1,1,4,4-tetracyanobuta-1,3-diene (TCBD) acceptor connected to a *N*,*N*-dialkylanilino or methoxyphenyl donor moiety. The dendrimer-like chromophores **5**–**7** feature three (**5** and **7**) or four (**6**) arrays of D–A dyads that are attached to a central benzene core. Derivative **7** includes 1,2-di(1,3-dithiol-2-ylidene)ethane-1,2-diyl fragments as donors, which are introduced by [2+2] cycloaddition between tetrathiafulvalene (TTF) and the electron-deficient triple bonds in **5**, followed by retro-electrocyclization.[7,11] The third class of compounds involves an electron-donating triphenylamine core to which D–A dyads are connected either by ethyne-1,2-diyl (in **8**) or 1-(buta-1,3-diyn-1-yl)-3,5-diethynylbenzene (in **9**) spacers.

Extensive X-ray crystallographic investigations on monomeric donor-substituted TCBDs, such as **1**–**3**,[6] showed that the chromophores are nonplanar, thereby impairing electron delocalization to a certain extent, and this should also hold for the more extended, multivalent systems **5**–**9**. Electrochemical investigations revealed that dendritic donor-substituted TCBDs undergo multiple redox steps at virtually matching potentials,[7] which suggests that the individual electron donor and acceptor moieties behave as independent electroactive centers.[12] This behavior has previously also been observed for ferrocenyl dendrimers by Astruc and co-workers[10] and by others.[13] Although these data suggest little communication between individual dyads in the multivalent systems, such as **5**–**9**, it was the aim of the present study to further quantify the extent of π-electron delocalization in radical anions and radical cations of **1**–**9** by means of EPR/ENDOR spectroscopy.

Synthesis: The syntheses of compounds **1**–**3**, **5**, and **7** have already been described.[6,7] Compounds **4** and **6** were obtained in near-quantitative yield by efficient cycloaddition of TCNE with the corresponding alkyne precursors, followed by in situ retro-electrocyclization, as previously reported. In the synthesis of the dendritic systems **8** and **9**, which feature a central triphenylamine core, sequences of iterative Sonogashira cross-couplings and silyl deprotections were applied.[14] Thus, triiodotriarylamine **10**[15] was cross-coupled with (trimethylsilyl)buta-1,3-diyne[16] to yield tris-alkynylated product **11**, which, after desilylation and cross-coupling with iodoarene **12**,[7] afforded dendritic **13** in 46% yield (Scheme 1). As desilylated **11** deteriorates readily even as a solution in THF to produce dark insoluble material, it must be subjected to subsequent reactions immediately (see the Supporting Information). Subsequent reaction of **13** with TCNE in CH_2Cl_2 at 20°C afforded the multivalent chromophore **9** in very high yield. All new donor-substituted TCBDs **4**, **6**, **8**, and **9** are deep-colored solids, stable at ambient temperature and when exposed to the laboratory atmosphere, and melt without decomposing above 100°C. The identity of the alkyne precursors such as **13** and the novel TCBD derivatives **4**, **6**, **8**, and **9** was confirmed by using ^{1}H and ^{13}C NMR spectroscopy and high-resolution MALDI-FT mass spectrometry and/or elemental analysis.

Radical anions: Generally, reduction of the parent molecules **1**–**9** with K or Zn metal in 1,2-dimethoxyethane (DME) and *N*,*N*-dimethylformamide (DMF) yielded EPR spectra that could be analyzed rather well. In some cases, EPR spectra could be obtained from the solutions of the parent compounds even before contact with the metal took place. These EPR spectra, however, were identical to those observed after a short contact of the reaction solutions with the metal mirror. Prolonged reductions led to the appearance of less-resolved EPR signals. The primary spectra were assigned to one-electron-reduced species, that is, to radical anions. One has to bear in mind that the experimental conditions and the sensitivity of EPR spectroscopy slightly differ from those of electrochemical experiments that indicate simultaneous multielectron transfers for the multivalent derivatives (see the Supporting Information, Table 1SI).[7]

One-electron reduction of **1** with K metal in DME yielded well-resolved and slightly temperature-dependent EPR spectra (Figure 1). A matching simulation of the experimental EPR spectrum was achieved by taking into account four almost equivalent ^{14}N nuclei with ^{14}N isotropic hyperfine coupling constants (hfc) of approximately 1 mT. The biggest hfc of 0.253 mT is attributed to the single proton at the C(3) position of the TCBD moiety. The phenyl protons and those of the methoxy substituent reveal spin populations with hfc values that are too small to be resolved in the EPR spectrum but distinguishable by ENDOR spectroscopy (see also the calculated values in Figure 1).

The EPR data obtained after reduction of **2** basically match those attributed to $\mathbf{1}^{\bullet-}$. A ^{14}N hfc of 0.109 mT is assigned to the four virtually equivalent N atoms of the TCBD unit. A one-proton hfc of 0.261 mT corresponds to the single alkene H atom, and an hfc of 0.029 mT can be allocated to the two equivalent *ortho* protons (with respect to the TCBD moiety) of the aryl substituent. Thus, it is not astonishing that the EPR spectra obtained for **1** and **2** indicate rather similar shapes and an identical number of lines (see Figure 1).

The EPR spectrum attributed to the radical anion $\mathbf{3}^{\bullet-}$, featuring two types of *N*,*N*-dimethylanilino (DMA) donors, one directly attached to the TCBD framework and the second through an acetylenic linker, can be simulated in a straightforward way by using one ^{14}N hfc of 0.114 mT for four virtually equivalent N atoms. Reduction of **4** with K in DME or

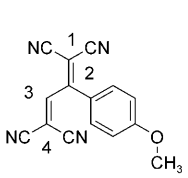

1

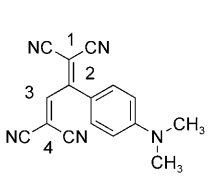

2

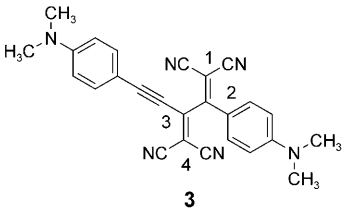

3

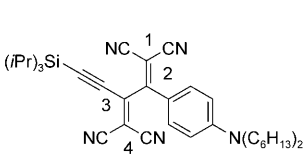

4

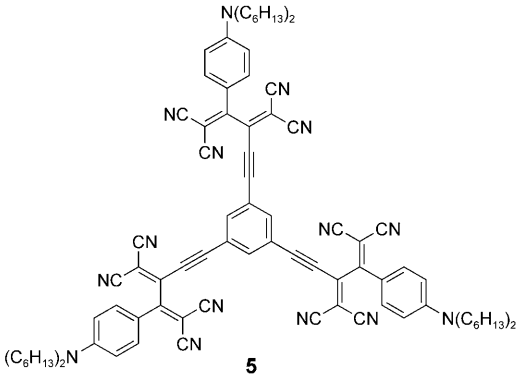

5

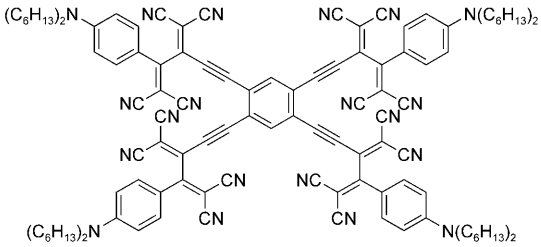

6

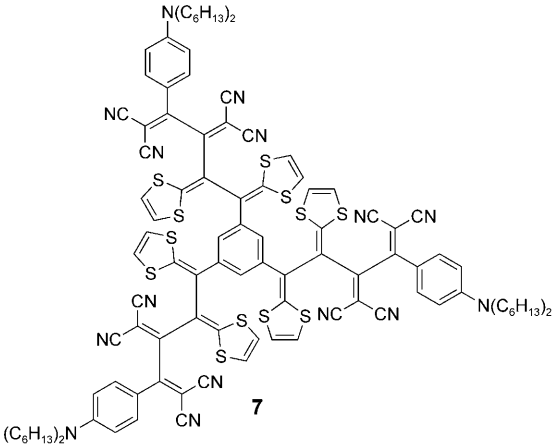

7

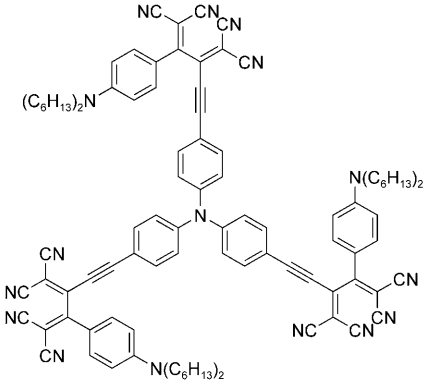

8

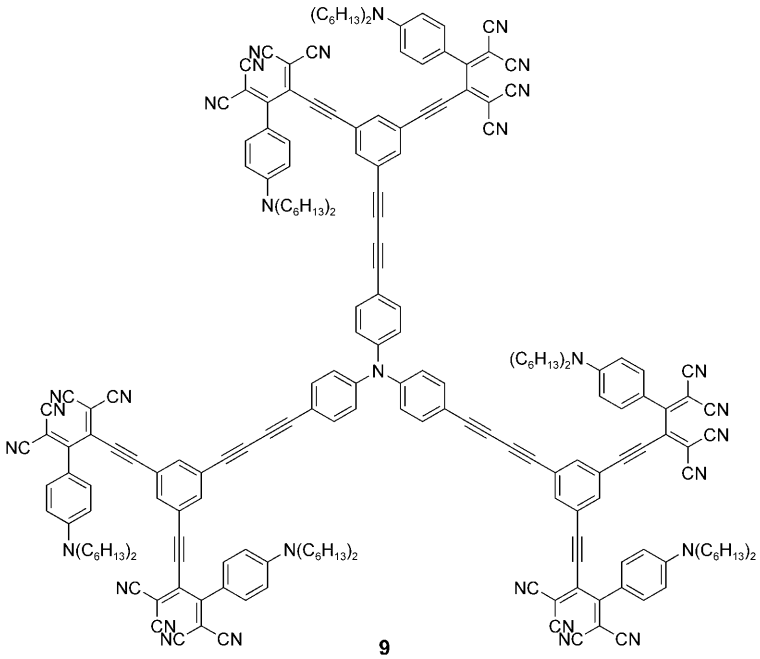

9

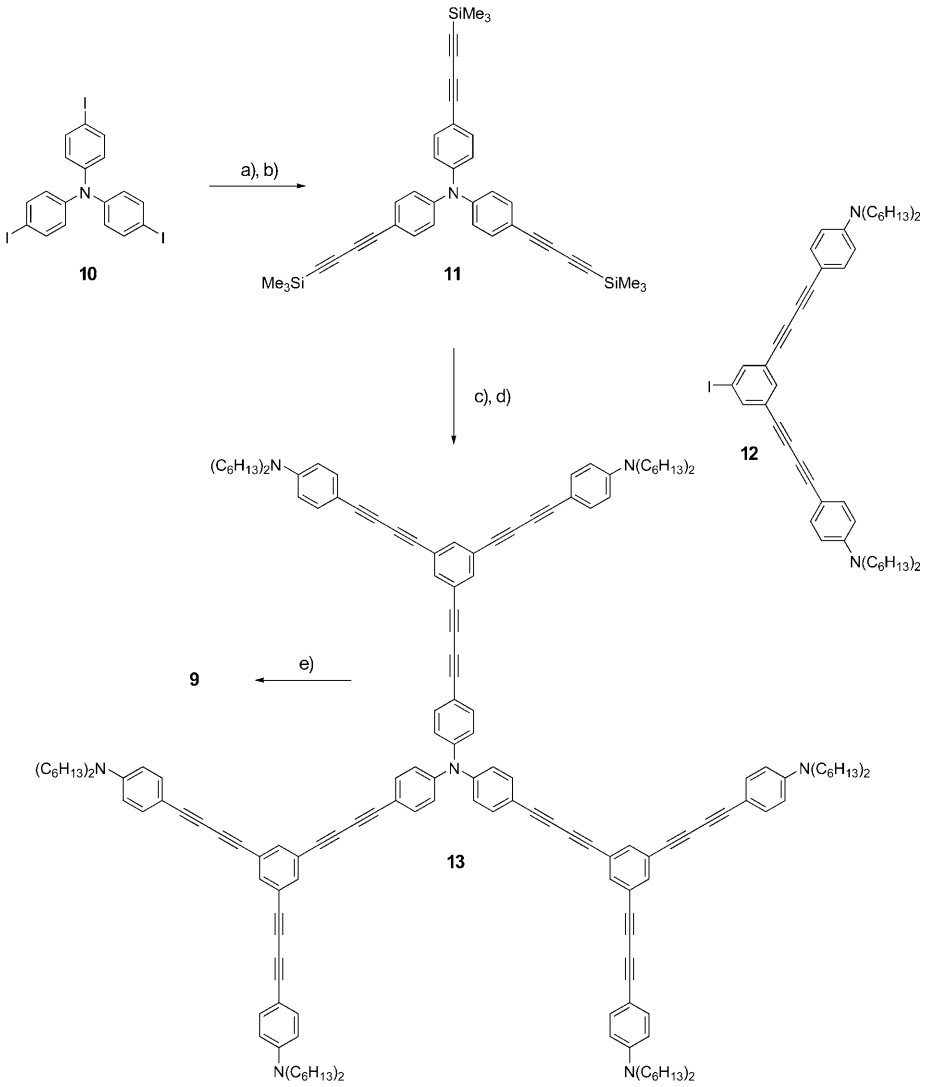

Scheme 1. Synthesis of dendritic charge-transfer chromophore **9**. a) 1,4-Bis(trimethylsilyl)buta-1,3-diyne, MeLi•LiBr, THF, 3 h, 20 °C, then H^+/H_2O; b) **10**, $[PdCl_2(PPh_3)_2]$, CuI, $(iPr)_2NH$, 13 h, 20 °C, 100 % (**11**) (yield over two steps). c) nBu_4NF, THF, 20 min, 0 °C. d) **12**, $[PdCl_2(PPh_3)_2]$, CuI, $(iPr)_2NH$, 15 h, 20 °C, 46 % (**13**) (yield over two steps). e) TCNE, CH_2Cl_2, 11 h, 20 °C, 100 % (**9**).

Zn in DMF led to unresolved EPR signals (Figure 2). Their width is compatible with those of $\mathbf{1}^{\bullet-}$, $\mathbf{2}^{\bullet-}$, and $\mathbf{3}^{\bullet-}$, thus the spin distribution in $\mathbf{4}^{\bullet-}$ is very likely to be similar to the former radical anions.

The EPR spectra assigned to $\mathbf{1}^{\bullet-}$, $\mathbf{2}^{\bullet-}$, $\mathbf{3}^{\bullet-}$, and $\mathbf{4}^{\bullet-}$ show that the character of the donor group at the phenyl substituent (methoxy in **1**, *N*,*N*-dialkylamino in **2**–**4**) does not significantly alter the spin distribution. The same electron distribution can also be established in derivatives **3** and **4**, in which the residual hydrogen atom on the TCBD moiety is replaced by either a 4-(*N*,*N*-dimethylamino)phenylethynyl or a (triisopropylsilyl)ethynyl group, respectively. With their well-defined electronic structure, radical anions $\mathbf{1}^{\bullet-}$ to $\mathbf{4}^{\bullet-}$ serve as ideal paradigms for the investigation of the multivalent derivatives **5**–**9** carrying multiple units of **4**.

The EPR data of $\mathbf{1}^{\bullet-}$ to $\mathbf{9}^{\bullet-}$are summarized together with the calculated hfc values in Table 1. In all cases, the ^{14}N hfc values are rather similar and in good agreement with their calculated counterparts. The ^1H hfc of H–C(3) in $\mathbf{1}^{\bullet-}$ and $\mathbf{2}^{\bullet-}$ amounts to approximately 0.25–0.26 mT, which demonstrates that spin transfer by means of this position is possible.[17] The remaining ^1H hfc values characterizing the amount of delocalization of the spin into the adjacent substituents are small, thus indicating that spin delocalization into the donor moieties is not significant. The shapes and the widths of EPR signals obtained for radical anions $\mathbf{3}^{\bullet-}$ to $\mathbf{9}^{\bullet-}$ are almost identical, pointing to very similar spin distributions in these charged species (Figure 2).

In conclusion, the EPR spectra attributed to $\mathbf{1}^{\bullet-}$ to $\mathbf{9}^{\bullet-}$ indicate that in the one-electron-reduced species, the spin and the charge are essentially confined to one 1,1,4,4-tetracyanobuta-1,3-dienyl moiety. There is no significant temperature dependence of the EPR spectral shape, thus dynamic phenomena such as spin transfer between identical acceptor units in $\mathbf{5}^{\bullet-}$ to $\mathbf{9}^{\bullet-}$on the hyperfine timescale can be ruled out.

According to the electrochemical measurements (see the Supporting Information),[7] simultaneous electron-transfer processes should take place upon reduction of dendritic **5**–**9**, impairing the observation of the primary radical anions $\mathbf{5}^{\bullet-}$ to $\mathbf{9}^{\bullet-}$. However, it has to be kept in mind that the experimental conditions applied in the electrochemical measurements and the environment in the diffusion layer at the working electrode are not identical to those of the EPR experiment. In the latter case, non-exhaustive reduction of the parent compound allows the formation of equilibria with EPR-detectable amounts of one-electron-reduced paramagnetic species, that is, the radical anions $\mathbf{1}^{\bullet-}$ to $\mathbf{9}^{\bullet-}$.

Radical cations: The starting point for describing the properties of the donor–acceptor molecules in this study are the radical cations of **2** and **4** because they resemble the electroactive unit in most of the derivatives introduced here (unexpectedly, oxidation of **1** did not yield any clearly distinguishable EPR spectra).

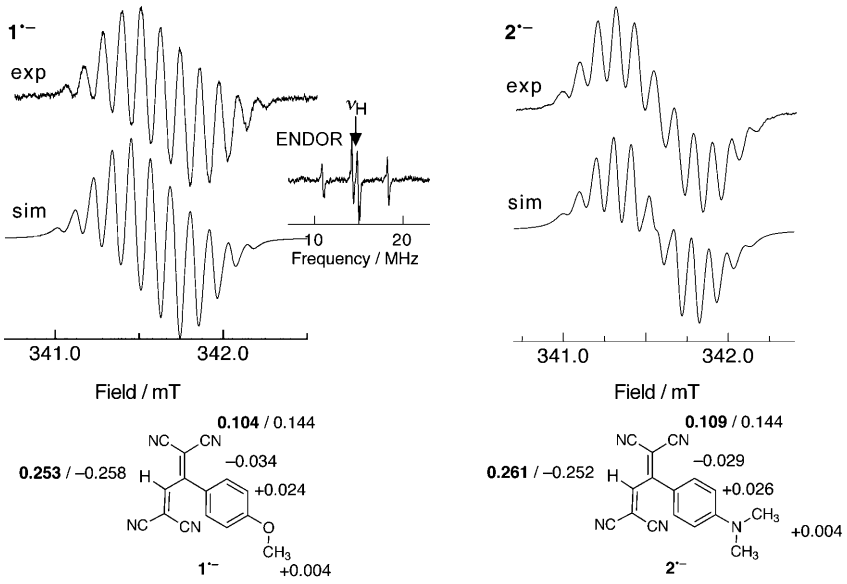

Figure 1. Experimental (exp) EPR spectra obtained after one-electron reduction of **1** ($T=280$ K) and **2** ($T=280$ K) with K metal in DME together with the corresponding simulations (sim). The experimental (bold) and calculated hfc values in mT and their assignments are displayed below the spectra. The inset shows the ENDOR spectrum of $\mathbf{1}^{\bullet-}$.

Oxidation of **2** with [bis(trifluoroacetoxy)iodo(III)]benzene (PIFA) in 1,1,1,3,3,3-hexafluoropropan-2-ol (HFP) or $AlCl_3$ in CH_2Cl_2 afforded a well-resolved EPR spectrum (Figure 3). The observed spectral pattern is produced by four different hfc values. The largest hfc of 1.36 mT can be assigned to the six equivalent β protons of the two methyl groups attached to the amino nitrogen atom. The smaller ^{1}H hfc values of 0.56 and 0.18 mT are attributed to the pairwise equivalent aromatic protons in the *ortho* and *meta* positions with respect to the *N*,*N*-dimethylamino substituent, respectively. These hfc values were verified by ENDOR spectroscopy. The EPR simulation reveals a ^{14}N hfc of 1.18 mT for the amino nitrogen atom. This spin distribution is in very good agreement with related alkyl-substituted aniline derivatives and forms the basis for the interpretation of the EPR spectra of the remaining molecules described herein.[18]

Silyl derivative **4** reveals an almost identical ^{14}N hfc (1.15 mT) as found in $\mathbf{2}^{\bullet+}$. The rather small ^{1}H hfc of 0.089 mT assigned to H−C(3) in $\mathbf{2}^{\bullet+}$ is missing, and additional hfc values attributable to the triisopropylsilyl group are not distinguishable. Importantly, the dominating six-proton hfc of approximately 1.3 mT in $\mathbf{2}^{\bullet+}$ is replaced by a lower ^{1}H hfc of 0.702 mT for the four equivalent β protons of the adjacent methylene groups in the *n*-hexyl substituents attached to the amino nitrogen atom (Table 2).

Remarkably, oxidation of **3** bearing two different DMA donor units leads to an EPR spectrum resembling that of $\mathbf{2}^{\bullet+}$ (Figure 3). The corresponding ^{14}N and the six methyl ^{1}H hfc values are not significantly lower than those for $\mathbf{2}^{\bullet+}$ (0.979 and 1.05 mT, respectively; Table 2). The remaining data resemble those of $\mathbf{2}^{\bullet+}$ as well. Thus, spin and charge are confined to only one DMA moiety. The above data show that the tendency of spin and charge delocalization from the DMA donor group attached to the TCBD acceptor in the 2-position is not pronounced. If a second donor moiety is attached as in **3** or **4**, hardly any spin is transferred to the second donor. This can be rationalized by the rather low ^{1}H hfc established for H−C(3) (0.089 mT) in **2**, indicating a low molecular orbital (MO) coefficient of the HOMO at this position (for calculated HOMO ($\mathbf{2}^{\bullet+}$) and LUMO ($\mathbf{2}^{\bullet-}$), see the Supporting Information, Figure 1SI). Generally, such low coefficients do not allow an efficient spin and charge transfer.[19]

This behavior is well reflected in the EPR spectra of dendritic radical cations $\mathbf{5}^{\bullet+}$ and $\mathbf{6}^{\bullet+}$. Their signals are rather similar (Figure 4), and the corresponding data closely resemble those of $\mathbf{4}^{\bullet+}$ (Table 2). Therefore, it can be concluded that one-electron oxidation of **5** and **6** by several methods (see the Experimental Section) leads to the formation of radical cations with the spin and the charge being confined to one *N*,*N*-dialkylanilino donor moiety.

Dendritic system **7** possesses 1,2-di(1,3-dithiol-2-ylidene)-ethane-1,2-diyl fragments (vinylogously extended tetrathiafulvalenes) as donors inserted between the central phenyl core and the peripheral DMA-substituted TCBD dyads. Not unexpectedly, only unresolved EPR signals could be detected after the oxidation of **7**. Their shape and the corresponding *g* factor (2.0060) are compatible with radical cations carrying the dominating amount of the spin and the charge at sulfur atoms. Unfortunately, we were not able to obtain ENDOR spectra of these species and can therefore not determine the amount of electron delocalization. Yet, it can be anticipated that the dominating amount of electron population resides at the 1,3-dithiol-2-ylidene moieties.[20] This is in very good agreement with the markedly lower first-oxidation potential of **7** (+0.41 V in CH_2Cl_2 versus Fc^+/Fc (ferricinium/ferrocene couple)) compared with **5** and **6** (+0.88 and +0.89 V in CH_2Cl_2 versus Fc^+/Fc, respectively; see the Supporting Information).[7] The first-oxidation potential of **7**, however, is considerably higher than that of **14**, which is approximately −0.30 V in MeCN (versus Fc^+/Fc) (Figure 5).[21] Thus, a considerable interaction of the vinylogous tetrathiafulvalene-type donor with the 1,1,4,4-tetracyanobuta-1,3-dienyl moiety exists. This is reasonable since the HOMO of **14** possesses rather

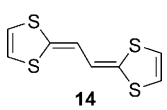

14

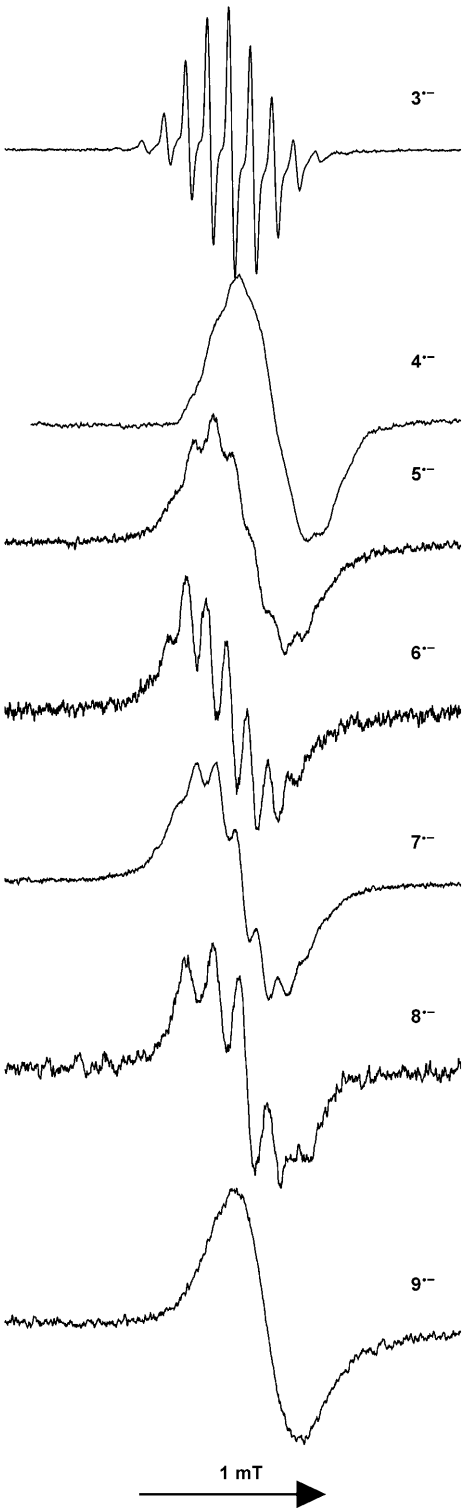

Figure 2. EPR spectra of $\mathbf{3}^{\bullet-}$ to $\mathbf{9}^{\bullet-}$ obtained by reduction with K metal in DME ($T = 260$–270 K).

Table 1. EPR data of radical anions $\mathbf{1}^{\bullet-}$ to $\mathbf{9}^{\bullet-}$ together with their calculated counterparts (UB3LYP/6-31G*) for $\mathbf{1}^{\bullet-}$, $\mathbf{2}^{\bullet-}$, and $\mathbf{3}^{\bullet-}$ (in italics).

	^{14}N hfc [mT] (4N)	^{1}H hfc [mT] (1H)	g factor
$\mathbf{1}^{\bullet-}$	0.104/*0.144*	0.253/*0.258*	2.0027
$\mathbf{2}^{\bullet-}$	0.109/*0.144*	0.261/*0.252*	2.0027
$\mathbf{3}^{\bullet-}$	0.117/*0.096*	–	2.0026
$\mathbf{4}^{\bullet-}$	0.13	–	2.0027
$\mathbf{5}^{\bullet-}$	0.092	–	2.0026
$\mathbf{6}^{\bullet-}$	0.109	–	2.0028
$\mathbf{7}^{\bullet-}$	0.107	–	2.0026
$\mathbf{8}^{\bullet-}$	0.136	–	2.0026
$\mathbf{9}^{\bullet-}$	[a]	–	2.0028

[a] Unresolved signal.

large MO coefficients at the central carbon atoms (see the Supporting Information, Figure 2SI).[21]

In dendritic **8** and **9**, which posses the oxidizable triphenylamine core, a competition between the oxidation of the central core and the peripheral *N*,*N*-dihexylanilino (DHA) substituents exists. The potential of the first three-electron oxidation of **8** centered at the DHA moieties (+0.89 V in CH_2Cl_2 versus Fc^+/Fc) is essentially identical to those of derivatives **2**, **5**, and **6** (see the Supporting Information; Figure 5).[6,7] Furthermore, a second one-electron oxidation step located on the central triphenylamine core in **8** was observed at +1.02 V. Indeed, immediately after oxidation of **8** with PIFA in HFP, an EPR spectrum similar to that assigned to $\mathbf{2}^{\bullet+}$, $\mathbf{5}^{\bullet+}$, and $\mathbf{6}^{\bullet+}$ is observed. However, this signal rapidly converts into a three-line spectrum reflecting one ^{14}N nucleus with an hfc of 0.89 mT (Figure 6). Presumably, the primary radical cation is rapidly converted to a triphenylamine-type radical cation under our experimental conditions. On the other hand, the first-oxidation potential of dendrimer **9** (+0.75 V versus Fc^+/Fc) is lower than those of derivatives **2**, **5**, and **6** and corresponds to the one-electron oxidation of the central triphenylamine core (see the Supporting Information). Thus, chemical oxidation of **9** with PIFA in HFP leads to the immediate appearance of a three-line EPR signal reflecting electron removal from the triphenylamine core.

The difference in the oxidation potentials of the central triphenylamine cores in **8** and **9** (+1.02 and +0.75 V versus Fc^+/Fc, respectively) might be explained in the following way: Upon introduction of the TCBD acceptor moieties, the oxidation potential of the triphenylamine core shifts to more positive potentials (the oxidation potential of triphenylamine is +0.39 V in MeCN versus Fc^+/Fc).[22] This shift is 630 mV in **8** and only 360 mV in the more extended **9**. The significantly smaller shift observed for **9** versus **8** is presumably due to the less-pronounced electron-withdrawing effect of the more distant TCBD units on the central triphenylamine core in **9** when compared with **8** (see the Supporting Information).

Conclusion

One-electron-reduced and -oxidized stages of D–A chromophores **1**–**9** (radical anions and radical cations, respectively), obtained by chemical reduction and oxidation of the corresponding neutral species, were studied by using EPR

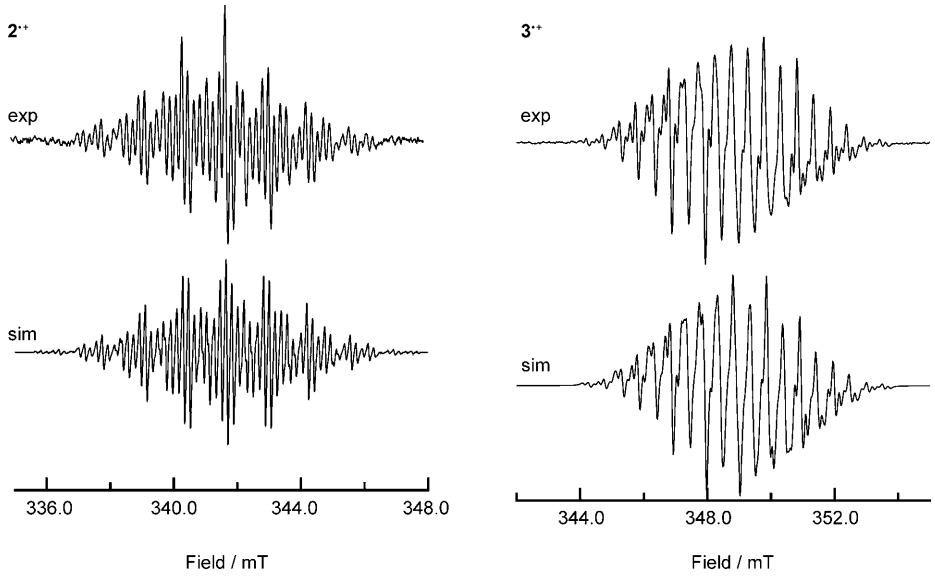

Figure 3. EPR spectra of $\mathbf{2}^{\bullet+}$ and $\mathbf{3}^{\bullet+}$ obtained by oxidation with PIFA in HFP ($T = 280$ K) together with their simulations.

Table 2. EPR data of radical cations $\mathbf{1}^{\bullet+}$–$\mathbf{9}^{\bullet+}$ together with their calculated counterparts (UB3LYP/6-31G*) for $\mathbf{2}^{\bullet+}$ and $\mathbf{3}^{\bullet+}$ (in italics; all hfc values in mT).

	^{14}N (amino)	^{1}H (H_β)[a]	^{1}H (H aromatic)[b]	*g* factor
$\mathbf{1}^{\bullet+}$	–	–	–	–
$\mathbf{2}^{\bullet+}$	1.18/*0.982* (1 N)	1.36/*1.18* (6 H)	0.56/*−0.53* (2 H, *o*) 0.18/*−0.21* (2 H, *m*)	2.0028
$\mathbf{3}^{\bullet+}$	0.98/*1.30* (1 N)	1.0/*0.775* (6 H)	0.49/*−0.26* (2 H, *o*) 0.17/*−0.09* (2 H, *m*)	2.0030
$\mathbf{4}^{\bullet+}$	1.15 (1 N)	0.70 (4 H)	0.54 (2 H, *o*)	2.0040
$\mathbf{5}^{\bullet+}$	1.17 (1 N)	0.70 (4 H)	0.52 (2 H, *o*)	2.0023
$\mathbf{6}^{\bullet+}$	0.98 (1 N)	0.52 (4 H)	0.43 (2 H, *o*)	2.0027
$\mathbf{7}^{\bullet+}$	–	–	–	2.0060
$\mathbf{8}^{\bullet+}$[a]	1.1 (1 N) 0.89 (1 N)	0.7 (4 H)	0.4 (2 H)	2.0030
$\mathbf{9}^{\bullet+}$	0.89 (1 N)	–	–	2.0030

[a] β Protons are separated from the spin-bearing $2p_z$-atom orbital by an sp^3-hybridized C atom. [b] The upper values represent the primary spectrum, those in the second line are consistent with the secondary spectrum, which is observed upon warming the sample (see the main text).

(ENDOR) spectroscopy. Although the MO coefficients in the LUMO would allow electron delocalization in radical anions $\mathbf{1}^{\bullet-}$ to $\mathbf{9}^{\bullet-}$, EPR investigations together with DFT calculations indicate that spin and charge are confined to the electron-withdrawing 1,1,4,4-tetracyanobuta-1,3-dienyl moiety on the hyperfine EPR timescale. The observed spin localization in $\mathbf{1}^{\bullet-}$ to $\mathbf{9}^{\bullet-}$ is presumably due to 1) substantial deviation of the π-system constituents from planarity as observed previously,[6] 2) limited π-electron delocalization, and very likely 3) counterion effects. An analogous spin and charge localization confined to the electron-donating *N*,*N*-dialkylaniline moieties is present in radical cations $\mathbf{2}^{\bullet+}$–$\mathbf{9}^{\bullet+}$; unexpectedly, oxidation of **1** did not yield any clearly distinguishable EPR spectra. In this case, delocalization is additionally impaired by rather small MO coefficients in the HOMO at the positions where the donor and acceptor moieties are linked.

These results suggest that highly charged stages of D–A chromophores **1**–**9** may display remarkable magnetic properties depending on the character of the environment (e.g., solvent, counterions, etc.). The exploration of these phenomena is now intensively being pursued.

Experimental Section

Materials and general methods: Reagents and solvents were purchased at reagent grade from Acros, Aldrich, and Fluka, and used as received. Tetrahydrofuran (THF) was freshly distilled from Na/benzophenone and CH_2Cl_2 from CaH_2 under N_2. All reactions were performed under an inert atmosphere by applying a positive pressure of N_2 or Ar. Column chromatography (CC) and plug filtrations were carried out with silica gel 60 (particle size 0.040–0.063 mm, 230–400 mesh; Fluka) and distilled technical solvents. Tris(4-iodophenyl)amine (**10**),[15] iodoarene **12**,[7] and *N*,*N*-dihexyl-4-[(triisopropylsilyl)buta-1,3-diyn-1-yl]aniline (**15**)[7] were prepared according to literature procedures. Thin-layer chromatography (TLC) was conducted on aluminum sheets coated with silica gel 60 F_{254} obtained from Macherey-Nagel; visualization with a UV lamp (254 or 366 nm). Melting points (m.p.) were measured on a Büchi B-540 melting-point apparatus in open capillaries and are uncorrected. "Decomp" refers to decomposition. ^{1}H and ^{13}C NMR spectra were measured on a Varian Gemini 300 or on a Bruker DRX500 spectrometer at 298 K unless otherwise stated. Chemical shifts (δ) are reported in ppm relative to the signal of tetramethylsilane (TMS). Residual solvent signals in the ^{1}H and ^{13}C NMR spectra were used as an internal reference. Coupling constants (J) are given in Hz. The apparent resonance multiplicity is described as s (singlet), brs (broad singlet), d (doublet), t (triplet), q (quartet), sept (septuplet), and m (multiplet). Infrared spectra (IR) were recorded on a Perkin–Elmer FT1600; signal designations: s (strong), m (medium), w (weak). UV/Vis spectra were recorded on a Varian Cary-5 spectrophotometer. The spectra were measured for samples in CH_2Cl_2 in a quartz cuvette (1 cm) at 298 K. The absorption maxima (λ_{max}) are reported in nm with the extinction coefficient (ε) in $M^{-1}cm^{-1}$ in brackets; shoulders are indicated as sh. High-resolution (HR) FT-ICR-MALDI spectra were measured on an IonSpec Ultima Fourier transform (FT) instrument with [(2*E*)-3-(4-*tert*-butylphenyl)-2-methylprop-2-enylidene]malononitrile (DCTB), or 3-hydroxypicolinic acid (3-HPA) as the matrix. The most important peaks are reported in m/z units with M as the molecular ion. MALDI-TOF spectra were recorded on a Bruker Daltonics Ultraflex mass spectrometer using DCTB as matrix. Elemental analyses were performed by the Mikrolabor at the Laboratorium für Organische Chemie, ETH Zürich, with a LECO CHN/900 instrument.

EPR and ENDOR measurements: EPR and ENDOR spectra were recorded on a Bruker ESP 300 spectrometer. The isotropic doublet EPR spectra were simulated with Winsim,[23] a public-domain program.

Sample preparation

Reductions: 1,2-Dimethoxyethane (DME) was heated to reflux over an Na/K alloy and stored over an Na/K alloy under high vacuum. DMF was stored over molecular sieves. All reductions were performed by contact

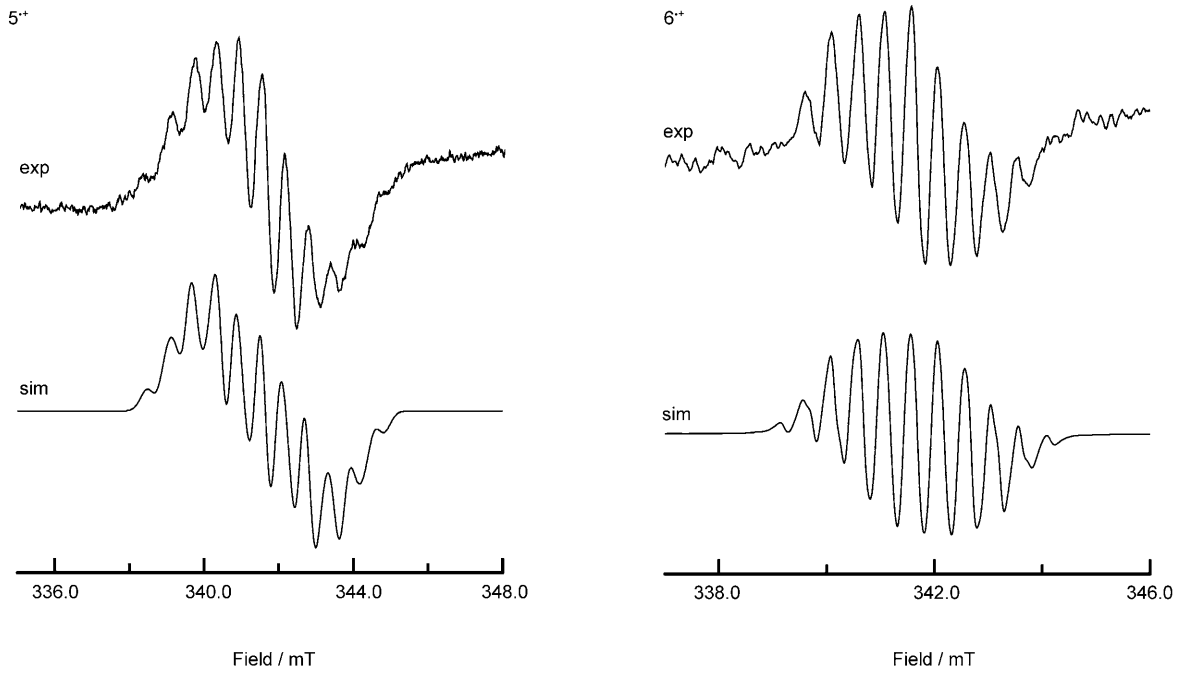

Figure 4. EPR spectra assigned to cations $\mathbf{5}^{\bullet+}$ and $\mathbf{6}^{\bullet+}$ obtained by oxidation with PIFA in HFP ($T=280$ K) together with their simulations.

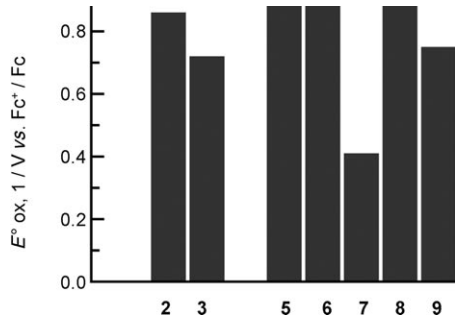

Figure 5. Comparison of the first-oxidation potentials of **2**,**3**, and **5**–**9**.

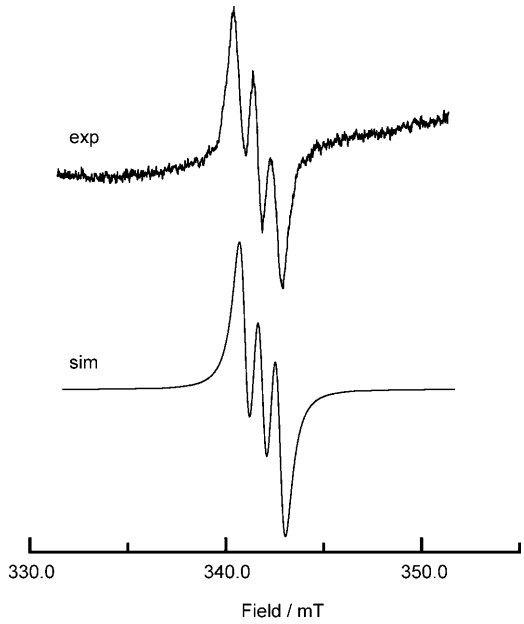

Figure 6. EPR spectrum of $\mathbf{8}^{\bullet+}$ obtained by oxidation with PIFA in HFP ($T=300$ K) together with its simulation.

of the solutions of the parent compounds with a K- or Zn-metal mirror under high vacuum.

Oxidations: CH_2Cl_2 was heated to reflux over molecular sieves and stored under high vacuum. 1,1,1,3,3,3-Hexafluoropropan-2-ol (HFP), trifluoroacetic acid (TFA), and [bis(trifluoroacetoxy)iodo(III)]benzene (PIFA) were purchased from Aldrich and used without further purification. Tris(4-bromophenyl)ammoniumyl hexachloroantimonate ("magic blue") was synthesized according to a literature procedure.[24] All oxidations were performed under high vacuum by reacting solutions of the oxidants in CH_2Cl_2 or HFP with those of the substrates. For oxidations in CH_2Cl_2, the solvent was distilled under high vacuum into the Pyrex-glass reaction cuvette charged with the oxidant and the substrate. The solutions in CH_2Cl_2 were stirred at 190 K (dry ice/2-propanol bath) and the sample was immediately transferred into the temperature-controlled microwave cavity of the EPR spectrometer. When HFP was used as the solvent, it was placed into the sample tube under Ar, sealed, and degassed by 3 or 4 freeze–pump–thaw cycles. The follow-up procedure was as described for CH_2Cl_2.

Calculations: Calculations were performed with the Gaussian 03 package.[25] For geometry optimization and single-point determinations of the Fermi contacts (hfc), the UB3LYP/6-31G* protocol was used. HOMOs and LUMOs for selected compounds were calculated by using the UB3LYP/6-31g(d) protocol and are shown in the Supporting Information.

2-[4-(Dihexylamino)phenyl]-3-[(triisopropylsilyl)ethynyl]buta-1,3-diene-1,1,4,4-tetracarbonitrile (4): A mixture of *N*,*N*-dihexyl-4-[(triisopropylsilyl)buta-1,3-diyn-1-yl]aniline (**15**) (100 mg, 0.22 mmol) and TCNE (27 mg, 0.22 mmol) in CH_2Cl_2 (30 mL) was stirred for 10 h at 20 °C. The solvent was evaporated under vacuum and the residue subjected to CC (silica gel, CH_2Cl_2) to give **4** (112 mg, 88 %) as a deep-purple solid. $R_f=0.67$ (silica gel, CH_2Cl_2); m.p. 124–126 °C; ^{1}H NMR (300 MHz, $CDCl_3$): $\delta=0.91$ (t, $J=6.6$ Hz, 6H), 1.07–1.10 (m, 21H), 1.33 (m, 12H), 1.63 (m,

4H), 3.39 (t, $J=7.8$ Hz, 4H), 6.67 (d, $J=9.4$ Hz, 2H), 7.72 ppm (d, $J=9.4$ Hz, 2H); ^{13}C NMR (75 MHz, $CDCl_3$): $\delta=11.21$, 14.18, 18.65, 22.78, 26.81, 27.44, 31.72, 51.63, 72.79, 96.70, 100.11, 110.17, 111.20, 112.18, 113.45, 114.64, 116.85, 126.39, 132.76, 151.09, 153.25, 159.56 ppm; IR (neat): $\tilde{\nu}=2928$ (m), 2864 (m), 2213 (s), 2140 (w), 1604 (s), 1543 (m), 1487 (s), 1449 (s), 1419 (s), 1349 (s), 1310 (m), 1262 (m), 1220 (s), 1187 (s), 1162 (s), 1116 (m), 1074 (w), 1022 (m), 999 (w), 883 (m), 828 (m), 803 cm^{-1} (m); UV/Vis (CH_2Cl_2): λ_{max} (ε) = 262 (13800), 311 (14500), 444 (25000), 468 (sh, 23000), 549 nm (sh, 7200 M^{-1}cm^{-1}); HR-MALDI-MS (3-HPA): m/z calcd for $C_{37}H_{52}N_5Si^+$ $[M+H]^+$: 594.3987; found: 594.3994; elemental analysis calcd (%) for $C_{37}H_{51}N_5Si$ (593.92): C 74.82, H 8.65, N 11.79; found: C 74.76, H 8.68, N 11.87.

2,2′,2″-[(5-{5,5-Dicyano-3-(dicyanomethylene)-4-[4-(dihexylamino)phenyl]pent-4-en-1-yn-1-yl}benzene-1,2,4-triyl)triethyne-2,1-diyl]tris{3-[4-(dihexylamino)phenyl]buta-1,3-diene-1,1,4,4-tetracarbonitrile} (6): A mixture of oligoalkyne **16** (50 mg, 0.038 mmol) and TCNE (20 mg, 0.153 mmol) in CH_2Cl_2 (25 mL) was stirred for 18 h at 20 °C. The solvent was evaporated under vacuum and the residue subjected to CC (silica gel, CH_2Cl_2/EtOAc 98:2) to give **6** (68 mg, 98 %) as a black metallic solid. $R_f=0.59$ (silica gel, CH_2Cl_2/EtOAc 98:2); m.p. 129–131 °C; ^{1}H NMR (300 MHz, $CDCl_3$): $\delta=0.91$ (t, $J=6.4$ Hz, 24H), 1.33 (s, 48H), 1.63 (m, 16H), 3.40 (t, $J=7.6$ Hz, 16H), 6.67 (d, $J=9.3$ Hz, 8H), 7.82 (d, $J=9.3$ Hz, 8H), 8.03 ppm (s, 2H); ^{13}C NMR (75 MHz, $CDCl_3$): $\delta=14.18$, 22.78, 26.81, 27.51, 31.68, 51.70, 71.60, 92.00, 98.81, 107.03, 109.93, 111.87, 112.53, 114.31, 114.78, 116.87, 125.61, 133.48, 139.26, 150.03, 153.79, 157.72 ppm; IR (neat): $\tilde{\nu}=2927$ (m), 2856 (m), 2213 (s), 2186 (m), 1600 (s), 1540 (m), 1484 (s), 1445 (s), 1414 (s), 1341 (s), 1262 (s), 1213 (s), 1182 (s), 1118 (s), 977 (m), 900 (m), 821 cm^{-1} (m); UV/Vis (CH_2Cl_2): λ_{max} (ε) = 287 (72100), 372 (138600), 471 (189900), 634 nm (19400 M^{-1}cm^{-1}); HR-MALDI-MS (3-HPA): m/z calcd for $C_{118}H_{123}N_{20}^+$ $[M+H]^+$: 1820.0234; found: 1820.0185; elemental analysis calcd (%) for $C_{118}H_{122}N_{20}$ (1820.40): C 77.86, H 6.75, N 15.39; found: C 77.97, H 7.01, N 15.10.

2,2′-{[(4-{5,5-Dicyano-3-(dicyanomethylene)-4-[4-(dihexylamino)phenyl]-pent-4-en-1-yn-1-yl}phenyl)imino]bis(4,1-phenyleneethyne-2,1-diyl)}bis{3-[4-(dihexylamino)phenyl]buta-1,3-diene-1,1,4,4-tetracarbonitrile} (8): A mixture of oligoalkyne **17** (50 mg, 0.043 mmol) and TCNE (33 mg, 0.257 mmol) in CH_2Cl_2 (30 mL) was stirred for 16 h at 20 °C. The solvent was evaporated under vacuum and the residue subjected to CC (silica gel, CH_2Cl_2/EtOAc 99:1) to give **8** (68 mg, 100 %) as a black solid. $R_f=0.55$ (silica gel, CH_2Cl_2/EtOAc 99:1); m.p. 122–126 °C; ^{1}H NMR (500 MHz, $CDCl_3$): $\delta=0.91$ (t, $J=6.9$ Hz, 18H), 1.32 (s, 36H), 1.61 (m, 12H), 3.37 (t, $J=7.9$ Hz, 12H), 6.66 (d, $J=9.4$ Hz, 6H), 7.10 (d, $J=8.8$ Hz, 6H), 7.57 (d, $J=8.8$ Hz, 6H), 7.75 ppm (d, $J=9.4$ Hz, 6H); ^{13}C NMR (125 MHz, $CDCl_3$): $\delta=13.96$, 22.57, 26.63, 27.27, 31.50, 51.46, 72.67, 87.10, 93.69, 110.34, 111.58, 112.08, 113.48, 114.53, 115.49, 116.77, 116.96, 124.58, 132.67, 135.41, 148.86, 150.65, 153.15, 159.25 ppm; IR (neat): $\tilde{\nu}=2925$ (m), 2855 (m), 2214 (m), 2160 (s), 1600 (s), 1483 (s), 1446 (s), 1412 (s), 1351 (s), 1317 (s), 1286 (s), 1211 (s), 1179 (s), 1116 (s), 1016 (m), 991 (m), 900 (w), 820 (m), 804 cm^{-1} (m); UV/Vis (CH_2Cl_2): λ_{max} (ε) = 279 (57500), 321 (sh, 52700), 347 (54500), 461 (157800), 522 nm (131100 M^{-1}cm^{-1}); HR-MALDI-MS (3-HPA): m/z calcd for $C_{102}H_{103}N_{16}^+$ $[M+H]^+$: 1551.8552; found: 1551.8582; elemental analysis calcd (%) for $C_{102}H_{102}N_{16}$ (1552.04): C 78.94, H 6.62, N 14.44; found: C 79.11, H 6.75, N 14.26.

2,2′,2″,2‴,2⁗,2⁗′-[Nitrilotris(4,1-phenylenebuta-1,3-diyne-4,1-diylbenzene-5,1,3-triyldiethyne-2,1-diyl)]hexakis{3-[4-(dihexylamino)phenyl]-buta-1,3-diene-1,1,4,4-tetracarbonitrile} (9): A mixture of **13** (16.0 mg, 0.006 mmol) and TCNE (12.5 mg, 0.097 mmol) in CH_2Cl_2 (20 mL) was stirred for 11 h at 20 °C. The solvent was evaporated under vacuum and the residue subjected to CC (silica gel, CH_2Cl_2/EtOAc 99:1) to give **9** (21 mg, 100 %) as a black solid. $R_f=0.53$ (silica gel, CH_2Cl_2/EtOAc 99:1); m.p. >130 °C (decomp); ^{1}H NMR (500 MHz, $CDCl_3$): $\delta=0.91$ (t, $J=6.5$ Hz, 36H), 1.34 (s, 72H), 1.64 (m, 24H), 3.40 (t, $J=7.8$ Hz, 24H), 6.70 (d, $J=9.3$ Hz, 12H), 7.06 (d, $J=8.7$ Hz, 6H), 7.46 (d, $J=8.7$ Hz, 6H), 7.75–7.78 (m, 15H), 7.85 ppm (d, $J=1.5$ Hz, 6H); ^{13}C NMR (125 MHz, $CDCl_3$): $\delta=13.96$, 22.57, 26.63, 27.28, 31.49, 51.52, 72.35, 73.25, 77.46, 78.10, 83.75, 86.08, 96.58, 109.79, 111.02, 111.35, 112.27, 113.52, 114.33, 116.06, 116.41, 121.21, 124.17, 124.75, 132.65, 134.16, 136.33, 139.15, 147.37, 150.31, 153.33, 158.12 ppm; IR (neat): $\tilde{\nu}=2925$ (m), 2855 (m), 2212 (m), 2186 (m), 1600 (s), 1533 (w), 1486 (s), 1446 (s), 1413 (s), 1339 (s), 1290 (m), 1212 (m), 1182 (s), 1117 (s), 1016 (w), 980 (w), 884 (m), 818 cm^{-1} (m); UV/Vis (CH_2Cl_2): λ_{max} (ε) = 288 (172000), 374 (236000), 414 (sh, 230000), 456 (272300), 568 nm (20800 M^{-1}cm^{-1}); HR-MALDI-MS (3-HPA): m/z calcd for $C_{216}H_{202}N_{31}^+$ $[M+H]^+$: 3231.6816; found: 3231.6722; elemental analysis calcd (%) for $C_{216}H_{201}N_{31}$ (3231.17): C 80.29, H 6.27, N 13.44; found: C 80.64, H 6.28, N 13.12.

Acknowledgements

This research was supported by the ETH Research Council, FWF (Austria, project no. P 20019-N17) and the NCCR "Nanoscale Science", Basel. Dr. Jean-Paul Gisselbrecht, Prof. Corinne Boudon, and Prof. Dr. Maurice Gross (Université Louis Pasteur, Strasbourg, France) are gratefully acknowledged for providing the electrochemical data of the new compounds and Dr. Carlo Thilgen (ETHZ) for his help with the nomenclature of the compounds described in this paper.

[1] For reviews on organic electronics and optoelectronics, see: a) Special Issue on "Organic Electronics" (Eds.: F. Faupel, C. Dimitrakopoulos, A. Kahn, C. Wöll): *J. Mater. Res.* **2004**, *19*, 1887–2203; b) T. W. Kelley, P. F. Baude, C. Gerlach, D. E. Ender, D. Muyres, M. A. Haase, D. E. Vogel, S. D. Theiss, *Chem. Mater.* **2004**, *16*, 4413–4422; c) *Acetylene Chemistry: Chemistry, Biology and Material Science* (Eds.: F. Diederich, P. J. Stang, R. R. Tykwinski), Wiley-VCH, Weinheim, **2005**; d) Special Issue on "Organic Electronics and Optoelectronics" (Eds.: S. R. Forrest, M. E. Thompson): *Chem. Rev.* **2007**, *107*, 923–1386; e) J. Roncali, P. Leriche, A. Cravino, *Adv. Mater.* **2007**, *19*, 2045–2060.

[2] For some recent work on conjugated electron donor–acceptor systems, see: a) F. B. Dias, S. Pollock, G. Hedley, L.-O. Pålsson, A. Monkman, I. I. Perepichka, I. F. Perepichka, M. Tavasli, M. R. Bryce, *J. Phys. Chem. B* **2006**, *110*, 19329–19339; b) M. M. Oliva, J. Casado, M. M. M. Raposo, A. M. C. Fonseca, H. Hartmann, V. Hernández, J. T. L. Navarrete, *J. Org. Chem.* **2006**, *71*, 7509–7520; c) C. Wang, L.-O. Pålsson, A. S. Batsanov, M. R. Bryce, *J. Am. Chem. Soc.* **2006**, *128*, 3789–3799; d) M. C. Díaz, B. M. Illescas, N. Martín, I. F. Perepichka, M. R. Bryce, E. Levillain, R. Viruela, E. Ortí, *Chem. Eur. J.* **2006**, *12*, 2709–2721; e) E. M. Priego, L. Sánchez, M. A. Herranz, N. Martín, R. Viruela, E. Ortí, *Org. Biomol. Chem.* **2007**, *5*, 1201–1209; f) E. L. Spitler, J. M. Monson, M. M. Haley, *J. Org. Chem.* **2008**, *73*, 2211–2223.

[3] For reviews on organic molecular conductors, see: a) Special Issue on "Molecular Conductors" (Ed.: P. Batail): *Chem. Rev.* **2004**, *104*, 4887–5782; b) T. Otsubo, K. Takimiya, *Bull. Chem. Soc. Jpn.* **2004**, *77*, 43–58; c) D. F. Perepichka, M. R. Bryce, *Angew. Chem.* **2005**, *117*, 5504–5507; *Angew. Chem. Int. Ed.* **2005**, *44*, 5370–5373; d) G. Saito, Y. Yoshida, *Bull. Chem. Soc. Jpn.* **2007**, *80*, 1–137.

[4] For some recent work on organic molecular conductors, see: a) Y. Morita, T. Murata, K. Fukui, S. Yamada, K. Sato, D. Shiomi, T. Takui, H. Kitagawa, H. Yamochi, G. Saito, K. Nakasuji, *J. Org. Chem.* **2005**, *70*, 2739–2744; b) T. Imakubo, M. Kibune, H. Yoshino, T. Shirahata, K. Yoza, *J. Mater. Chem.* **2006**, *16*, 4110–4116; c) T. Murata, Y. Morita, Y. Yakiyama, K. Fukui, H. Yamochi, G. Saito, K. Nakasuji, *J. Am. Chem. Soc.* **2007**, *129*, 10837–10846.

[5] a) N. N. P. Moonen, W. C. Pomerantz, R. Gist, C. Boudon, J.-P. Gisselbrecht, T. Kawai, A. Kishioka, M. Gross, M. Irie, F. Diederich, *Chem. Eur. J.* **2005**, *11*, 3325–3341; b) F. Bureš, W. B. Schweizer, J. C. May, C. Boudon, J.-P. Gisselbrecht, M. Gross, I. Biaggio, F. Diederich, *Chem. Eur. J.* **2007**, *13*, 5378–5387.

[6] a) T. Michinobu, J. C. May, J. H. Lim, C. Boudon, J.-P. Gisselbrecht, P. Seiler, M. Gross, I. Biaggio, F. Diederich, *Chem. Commun.* **2005**, 737–739; b) T. Michinobu, C. Boudon, J.-P. Gisselbrecht, P. Seiler, B. Frank, N. N. P. Moonen, M. Gross, F. Diederich, *Chem. Eur. J.* **2006**, *12*, 1889–1905.

[7] M. Kivala, C. Boudon, J.-P. Gisselbrecht, P. Seiler, M. Gross, F. Diederich, *Angew. Chem.* **2007**, *119*, 6473–6477; *Angew. Chem. Int. Ed.* **2007**, *46*, 6357–6360.
[8] a) M. I. Bruce, J. R. Rodgers, M. R. Snow, A. G. Swincer, *J. Chem. Soc. Chem. Commun.* **1981**, 271–272; b) C. Cai, I. Liakatas, M.-S. Wong, M. Bösch, C. Bosshard, P. Günter, S. Concilio, N. Tirelli, U. W. Suter, *Org. Lett.* **1999**, *1*, 1847–1849; c) X. Wu, J. Wu, Y. Liu, A. K.-Y. Jen, *J. Am. Chem. Soc.* **1999**, *121*, 472–473; d) Y. Morioka, N. Yoshizawa, J.-i. Nishida, Y. Yamashita, *Chem. Lett.* **2004**, *33*, 1190–1191.
[9] J. C. May, P. R. LaPorta, B. Esembeson, I. Biaggio, T. Michinobu, F. Bureš, F. Diederich, *Proc. SPIE-Int. Soc. Opt. Eng.* **2006**, *6331*, 633101/1–633101/14.
[10] a) S. Nlate, J. Ruiz, V. Sartor, R. Navarro, J.-C. Blais, D. Astruc, *Chem. Eur. J.* **2000**, *6*, 2544–2553; b) J. Ruiz, C. Pradet, F. Varret, D. Astruc, *Chem. Commun.* **2002**, 1108–1109; c) M.-C. Daniel, J. Ruiz, J.-C. Blais, N. Daro, D. Astruc, *Chem. Eur. J.* **2003**, *9*, 4371–4379.
[11] a) H. Hopf, M. Kreutzer, P. G. Jones, *Angew. Chem.* **1991**, *103*, 1148–1149; *Angew. Chem. Int. Ed. Engl.* **1991**, *30*, 1127–1128; b) G. Schermann, O. Vostrowsky, A. Hirsch, *Eur. J. Org. Chem.* **1999**, 2491–2500.
[12] J. B. Flanagan, S. Margel, A. J. Bard, F. C. Anson, *J. Am. Chem. Soc.* **1978**, *100*, 4248–4253.
[13] a) V. J. Chebny, D. Dhar, S. V. Lindeman, R. Rathore, *Org. Lett.* **2006**, *8*, 5041–5044; b) K. Hosomizu, H. Imahori, U. Hahn, J.-F. Nierengarten, A. Listorti, N. Armaroli, T. Nemoto, S. Isoda, *J. Phys. Chem. C* **2007**, *111*, 2777–2786.
[14] R. Chinchilla, C. Nájera, *Chem. Rev.* **2007**, *107*, 874–922.
[15] M. J. Plater, T. Jackson, *J. Chem. Soc. Perkin Trans. 1* **2001**, 2548–2552.
[16] V. Fiandanese, D. Bottalico, G. Marchese, A. Punzi, *Tetrahedron* **2004**, *60*, 11421–11425.
[17] a) M. Baumgarten, L. Gherghel, S. Karabunarliev, *Synth. Met.* **1995**, *69*, 633–636; b) U. Müller, M. Baumgarten, *J. Am. Chem. Soc.* **1995**, *117*, 5840–5850; c) G. Zhou, M. Baumgarten, K. Müllen, *J. Am. Chem. Soc.* **2007**, *129*, 12211–12221.
[18] F. Gerson, W. Huber, *Electron Spin Resonance Spectroscopy of Organic Radicals*, Wiley-VCH, Weinheim, **2003**.
[19] B. Grossmann, J. Heinze, T. Moll, C. Palivan, S. Ivan, G. Gescheidt, *J. Phys. Chem. B* **2004**, *108*, 4669–4672.
[20] H. Hopf, M. Kreutzer, C. Mlynek, M. Scholz, G. Gescheidt, *Helv. Chim. Acta* **1994**, *77*, 1466–1474.
[21] T. Sugimoto, H. Awaji, I. Sugimoto, Y. Misaki, T. Kawase, S. Yoneda, Z.-i. Yoshida, T. Kobayashi, H. Anzai, *Chem. Mater.* **1989**, *1*, 535–547.
[22] E. T. Seo, R. F. Nelson, J. M. Fritsch, L. S. Marcoux, D. W. Leedy, R. N. Adams, *J. Am. Chem. Soc.* **1966**, *88*, 3498–3503.
[23] D. R. Duling, NIEHS, Research Triangle Park, NC, USA, **1995**.
[24] F. A. Bell, A. Ledwith, D. C. Sherrington, *J. Chem. Soc. C* **1969**, 2719–2720.
[25] Gaussian 03 (Revision C.02), M. J. Frisch, G. W. Trucks, H. B. Schlegel, G. E. Scuseria, M. A. Robb, J. R. Cheeseman, J. A. Montgomery, Jr., T. Vreven, K. N. Kudin, J. C. Burant, J. M. Millam, S. S. Iyengar, J. Tomasi, V. Barone, B. Mennucci, M. Cossi, G. Scalmani, N. Rega, G. A. Petersson, H. Nakatsuji, M. Hada, M. Ehara, K. Toyota, R. Fukuda, J. Hasegawa, M. Ishida, T. Nakajima, Y. Honda, O. Kitao, H. Nakai, M. Klene, X. Li, J. E. Knox, H. P. Hratchian, J. B. Cross, V. Bakken, C. Adamo, J. Jaramillo, R. Gomperts, R. E. Stratmann, O. Yazyev, A. J. Austin, R. Cammi, C. Pomelli, J. W. Ochterski, P. Y. Ayala, K. Morokuma, G. A. Voth, P. Salvador, J. J. Dannenberg, V. G. Zakrzewski, S. Dapprich, A. D. Daniels, M. C. Strain, O. Farkas, D. K. Malick, A. D. Rabuck, K. Raghavachari, J. B. Foresman, J. V. Ortiz, Q. Cui, A. G. Baboul, S. Clifford, J. Cioslowski, B. B. Stefanov, G. Liu, A. Liashenko, P. Piskorz, I. Komaromi, R. L. Martin, D. J. Fox, T. Keith, M. A. Al-Laham, C. Y. Peng, A. Nanayakkara, M. Challacombe, P. M. W. Gill, B. Johnson, W. Chen, M. W. Wong, C. Gonzalez, J. A. Pople, Gaussian, Inc., Wallingford CT, **2004**.

Received: April 15, 2008
Published online: July 18, 2008

